# Spectro-electrochemical studies of single wall carbon nanotubes films

P. Corio [a,*], A. Jorio [b], N. Demir [c], M.S. Dresselhaus [d]

[a] *Instituto de Química, Universidade de São Paulo, Av. Prof. Lineu Prestes 748, São Paulo 05508-900, Brazil*
[b] *Departamento de Física, Universidade Federal de Minas Gerais, Belo Horizonte 30123-970, Brazil*
[c] *Department of Physics, Massachusetts Institute of Technology, Cambridge, MA 02139-4307, USA*
[d] *Department of Physics and Department of Electrical Engineering and Computer Science, Massachusetts Institute of Technology, Cambridge, MA 02139-4307, USA*

## Abstract

The dependence of the resonance Raman spectra of single wall carbon nanotubes (SWNTs) on an externally applied potential ($V_{ap}$) was studied in different media. The spectro-electrochemical data indicate that the reaching of van Hove singularities (vHSs) of SWNTs occurs at a different $V_{ap}$ for each electrolyte, and that there is a dependence of the charge transfer and intercalation processes on the chemical nature of the media. We present evidence to suggest that the position of the vHSs of SWNTs is perturbed by $V_{ap}$. Asymmetry between empty and filled vHSs is revealed by the spectroscopic response upon electrochemical p- and n-doping.
© 2004 Elsevier B.V. All rights reserved.

## 1. Introduction

Single wall carbon nanotube (SWNT) properties can be appreciably altered by different kinds of chemical interactions, such as electrochemical or chemical charge transfer processes. The electrochemical modification of the behavior of SWNT bundles has been a subject of recent interest [1–5]. The doping of nanotubes, via a chemical or electrochemical process can be used to influence their electronic structure, since it can modify the populations of van Hove singularities (vHSs) in the 1 D electronic density of states [6]. Thus, electron transfer processes in SWNT samples lead to a significant modification of their vibrational and electronic properties.

Advances in Raman spectroscopy studies on isolated carbon nanotubes recently allowed the study of the electrochemical gating of individual carbon SWNTs [7], where sharp increases in current through metallic nanotubes with electrochemical gate voltages were demonstrated, indicating that the Fermi energy passes through valence and conduction band vHSs.

In the present work, Raman scattering of metallic and semiconducting SWNTs bundles are measured at different applied electrochemical potentials in different chemical environments in order to explore the effects of counterions in the doping processes of nanotubes. The effect of p-type and n-type doping of SWNT bundles on the electronic structure of the nanotubes is investigated by in situ resonance Raman spectroscopy.

## 2. Experimental

The Raman spectra were acquired on a Renishaw Raman System 3000 equipped with an Olympus microscope (BTH2) and with an 80×objective to focus the laser beam on the sample. For excitation radiation, the 632.8 nm line from an air cooled He–Ne laser was used. This laser line allows for resonance with metallic nanotubes. The experiments were performed under ambient conditions using a back-scattering geometry.

The working electrode was a platinum electrode with a 0.2 cm$^2$ geometrical area. A thin film of SWNT bundles was deposited on the metal surface from a sonicated dispersion of nanotubes in acetonitrile or isopropyl alcohol. The in situ Raman spectra were recorded, while

---

varying the applied potential in steps of 0.1 V. All the potentials are referred to an Ag/AgCl reference electrode. The electrochemical system was a PAR 263 potentiostat/galvanostat from EG&G.

The SWNTs used in this work were produced by the electric arc discharge method. A catalyst with a 1:1 Ni:Co atomic ratio was used in the synthesis. The diameter distribution of this sample was determined to be $d_0 = 1.25 \pm 0.20$ nm by analysis of the laser excitation energy dependence of the tangential G-band phonon modes [8].

The chemicals and solvents were supplied by Aldrich and Merck. All chemicals were analytical grade and were used as received without any further purification. The electrolyte solutions were prepared using analytical grade chemicals and doubly distilled water. The organic solvents were spectroscopic grade.

## 3. Results and discussion

Studies of various cathodic and anodic polarization effects of carbon nanotubes under different conditions will now be discussed in terms of changes in the Raman spectra with regard to the charge transfer process in different electrolytes and the reversibility of the application of an external potential.

### 3.1. Oxidation of a SWNT film in an HNO₃ media

The electrochemical oxidation of a SWNTs thin film on a platinum surface in an HNO₃ aqueous solution was investigated by taking a Raman spectrum at constant applied potential $V_{ap}$ for several values of $V_{ap}$ in the range between 0.0 and 1.4 V. After the scans at all the non-zero $V_{ap}$ were taken, the spectrum at 0.0 V was once again taken, and this spectrum is also presented in Fig. 1 for comparison with the initial spectrum taken at $V_{ap} = 0.0$ V.

Fig. 1 shows that a strong variation of the Raman features occurs with increasing applied potential $V_{ap}$. The frequency upshift of the tangential G-band and of the dispersive G'-mode frequencies are associated with the removal of electrons from the SWNT π-band, as previously reported in the study of the electrochemical oxidation of nanotubes in an H₂SO₄ medium [1,5].

The Breit–Wigner–Fano (BWF) contribution to the tangential mode also decreases significantly, as a consequence of the decrease in electronic density and therefore of the electron–phonon coupling effect in metallic nanotubes. In fact, it has been suggested that the plasmon coupling between tubes controls the intensity of the BWF contribution to the G-band for metallic tubes [9]. The movement of the Fermi level directly changes the charge density in metallic tubes and therefore should sensitively affect the BWF intensity. The
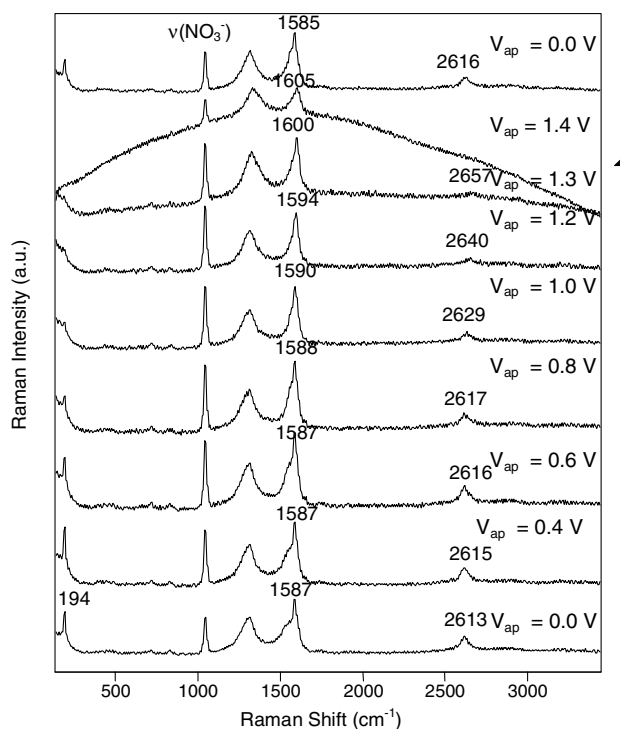


Fig. 1. In situ Raman spectra of a SWNT film cast on a platinum surface in HNO₃ 0.5 mol L$^{-1}$ aqueous solution obtained at the indicated applied potentials. $E_{laser} = 1.96$ eV. The arrow on the right indicates the order in which the traces were taken.

results presented here based on variation of $V_{ap}$ may provide a sensitive experimental probe of plasmon effects in SWNT bundles.

The RBM feature, located at ca. 194 cm$^{-1}$, shows a peculiar behavior. While its frequency varies very little with the applied potential, its intensity is particularly sensitive to $V_{ap}$ and decreases rapidly with more positive potentials. It is interesting to observe that the intensity of the RBM feature essentially vanishes for $V_{ap}$ more positive than 1.0 V. This indicates that the electrons that were in the filled valence band vHS $E_1^M$, and were involved in the resonant electronic transition have been removed, resulting in the loss of the resonance Raman condition. These data are in good agreement with the results in [5]. The diameter of a SWNT can be directly estimated from the frequency of its RBM band [10], according to the expression $\omega_{RBM} = 248$ cm$^{-1}/d_t$. In Fig. 1, the RBM is observed at 194 cm$^{-1}$, which corresponds to a nanotube with a diameter of ca. 1.28 nm. According to results calculated for the energy separations $E_{ii}(d_t)$ between vHSs for SWNTs obtained from tight-binding calculations [11], favorable conditions for the resonance of metallic tubes for $E_{laser} = 1.96$ eV should occur for diameters in the $1.2 < d_t < 1.35$ nm range.

The results in Fig. 1 also show that up to 1.4 V, the oxidation process can be considered to be reversible,

since, although some minor changes occur, the main features of the Raman spectrum are recovered when the potential is returned to 0.0 V (RBM, G and G′ bands).

## 3.2. Electrochemistry in $K_2SO_4$: study of the oxidation and reduction processes

Since the effect of applying negative potentials in acid media cannot be properly investigated due to the evolution of hydrogen, the effect of both anodic and cathodic applied potentials was then investigated in a $K_2SO_4$ 0.5 M aqueous solution, as shown in Fig. 2.

### 3.2.1. The effect of anodic polarization (p doping)
Fig. 2a shows the oxidation of nanotubes on a platinum electrode in $K_2SO_4$ aqueous solution. The spectro-electrochemical behavior is generally similar to that
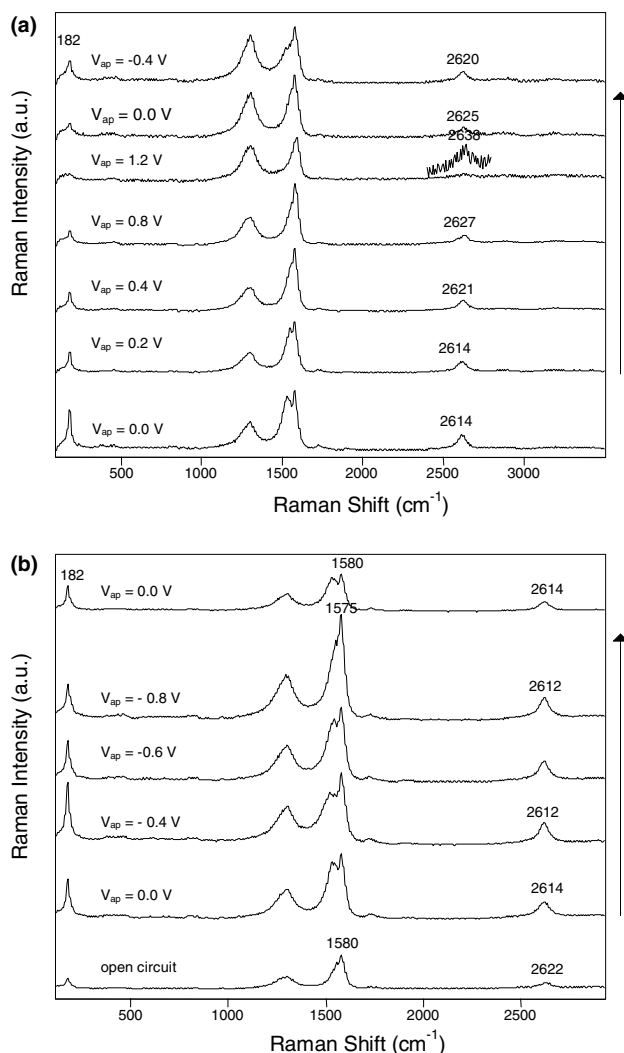


Fig. 2. In situ Raman spectra of a SWNT film cast on a platinum surface in $K_2SO_4$ 0.5 mol $L^{-1}$ aqueous solution obtained at (a) anodic and (b) cathodic polarization. $E_{laser} = 1.96$ eV. The arrow on the right indicates the order in which the traces were taken.

observed in $H_2SO_4$ and $HNO_3$ media – i.e., the spectral changes are related to the oxidation process of the nanotubes. This oxidation can be considered to be a quasi-reversible process. As can be seen by the careful observation of the spectra in Fig. 2a, when $V_{ap}$ is returned to 0.0 V after applying +1.2 V, the resulting spectrum shows some differences as compared to the initial spectrum for $V_{ap} = 0.0$ V. Specifically, the RBM feature shows a smaller intensity, and the G′-band is significantly upshifted in comparison to the initial $V_{ap} = 0.0$ V spectrum. In fact, the spectrum obtained for $V_{ap} = 0.0$ V after the oxidation of the SWNTs bundles is very similar (in frequencies and relative intensities) to the spectra initially observed for $V_{ap} = 0.8$ V. In trying to restore the initial electronic density of the nanotubes and to recover the initial $V_{ap} = 0.0$ V spectrum, we have applied more negative potentials, as shown in Fig. 2a for $V_{ap} = -0.4$ V. Even after this considerably negative $V_{ap}$ excursion, the spectrum at $V_{ap} = 0.0$ V differs from the initial one for the unperturbed sample, best resembling the initial spectrum at $V_{ap} = 0.4$ V. This demonstrated a significant hysteresis – related to going to too high a value of $V_{ap}$ (e.g. + 1.2 V) – in the doping and undoping of nanotubes.

### 3.2.2. The effect of cathodic polarization (n doping)
The spectro-electrochemistry of SWNTs on a platinum electrode in a $K_2SO_4$ electrolytic solution for negative values of $V_{ap}$ is shown in Fig. 2b. The spectra could only be measured up to $V_{ap} = -0.8$ V, since the use of $V_{ap}$ more negative than $-0.8$ V produces $H_2$ evolution from the electrochemical decomposition of water.

The first spectrum in Fig. 2b was obtained at open circuit potential (OCP), i.e. no external electrochemical potential was applied. In this case, the open circuit potential corresponds to 0.35 V, as measured by the equilibrium cell potential. In fact, this spectrum at open circuit potential is similar to the spectrum at $V_{ap} = 0.4$ V in Fig. 2a, that was taken just before. It is interesting that, after applying 0.0 V, the Raman signal is enhanced. The tangential G-band mode reflects the metallic modes more clearly, the G′-mode band is downshifted by ca. 8 $cm^{-1}$, and the RBM is significantly enhanced, as compared to the tangential modes (see Fig. 2b). At ca. $-0.4$, it seems that the best resonance conditions with metallic tubes is achieved.

In the discussion of the results obtained above, we have assumed, as a first approximation, that the position of the vHSs would not be perturbed by the external applied potential. It has been assumed that the dominant effect of changing $V_{ap}$ would be to either add electrons to an empty vHS or to remove electrons from a filled vHS. In both cases, the ability of the nanotubes to undergo an optical transition with a resonant photon decreases. This would account for the decrease in the resonant Raman condition as an external field is applied. In fact, it has

been previously observed that when a SWNT electrode is polarized anodically or cathodically, the main effect is a reversible bleaching of the optical electronic transitions between vHSs and a reversible quenching of resonance Raman scattering [2,6,12]. However, the results in Fig. 2 show that, depending on specific experimental conditions (such as the diameter distribution of SWNTs and the chemical environment), by applying an external voltage to the SWNT film, the Raman cross section for the nanotubes for a particular laser excitation energy can actually increase. This suggests that the energies of the van Hove singularities are in fact being significantly perturbed by the applied potential, so that the $E_{11}^{M}$ transition energy is changed. In this way, the modified transition energy shows a better resonance with the incident laser photon, resulting in an enhancement of the observed Raman cross section.

In order to better analyze the differences between the spectrum obtained under open circuit conditions and the spectrum obtained with a polarization of the electrode, we show in Fig. 3 the subtraction spectrum, obtained when the spectrum at open circuit is subtracted from the spectrum at 0.0 V. This approach allows the clear observation of the vibrational modes that are enhanced by applying voltage to the working electrode. The insert shows the bandshape analysis of the tangential mode band obtained by the described subtraction. This tangential mode band shows the characteristic frequencies assigned to metallic nanotubes. So, by applying an external electrochemical potential, *the resonance condition for metallic tubes* in this sample for $E_{laser} = 1.96$ eV is enhanced. Thus, the signal shown in Fig. 3 strongly emphasizes the Raman spectrum of a particular diameter nanotube that is brought into resonance by $V_{ap}$.

As $V_{ap}$ reaches −0.8 V in Fig. 2b, and the Fermi level of the SWNTs is increased, the Raman spectra become

more typical of semiconducting SWNTs. This is an indication that for $V_{ap} = -0.8$ V, $E_F$ has passed through the valence band $E_{11}^{M}$ for most of the SWNTs in this sample, resulting in the quenching of the Raman scattering corresponding to the metallic tubes. This would explain the relative decrease in the RBM feature as compared to the tangential G-band, since the most prominent RBM Raman band is observed at 182 cm$^{-1}$, corresponding to a metallic nanotube with a diameter of 1.36 nm. The relatively enhanced tangential G-band can be assigned to the presence of semiconducting tubes in the sample, mostly in resonance with $E_{33}^{S}$ for $E_{laser} = 1.96$ eV and having larger diameters.

Fig. 2b also shows the Raman signal obtained for $V_{ap} = 0.0$ V after the negative voltage scan, for comparison with the initial spectrum taken at $V_{ap} = 0.0$ V. Although the final spectrum (top trace) shows a somewhat lower intensity than the initial one (lower trace), the frequencies and relative intensities of the Raman bands are very similar. The electrochemical charge transfer process in this case can, therefore, be considered to be reversible.

It is also important to observe in Fig. 2 that the effect of increasing and decreasing the Fermi level of SWNTs is not symmetrical. This effect may result from a small asymmetry between the positions of empty and filled vHSs in the SWNT electronic density of states. Most studies of carbon nanotubes to date have assumed that the energies of the vHSs for the empty and filled states are symmetrical [11]. Future detailed studies, which quantitatively separate the dominant dependence of the electrochemical potential from the smaller dependence of the vHS energies on $V_{ap}$ will have the ability to reveal the asymmetry between the filled and empty states quantitatively.

The voltage dependence of the absolute intensities of the most important features in the Raman spectra of SWNTs over a broad range of applied potentials is shown in Fig. 4. More significant intensity changes occur for the tangential G-mode and for the RBM as compared to the G′-mode. It is also interesting to note the very different behavior observed by the intensity enhancement patterns for the tangential G-mode and for the RBM. While the G-mode shows a minimum intensity at $V_{ap} = -0.2$ V, the RBM shows a maximum for the same voltage. This demonstrates that different vibrational modes have different resonance enhancement patterns, indicating that the changes in the $E_F$ positions affect the Raman cross section of different vibrational modes in a different way: the RBM and tangential G-mode tend to behave very differently; and the intensity of the G′-mode is less affected. While the G′-mode changes significantly in frequency due to the softening or hardening of the C–C bond, it varies very little in absolute intensity. Therefore, all Raman features increase/decrease in intensity as the best resonance
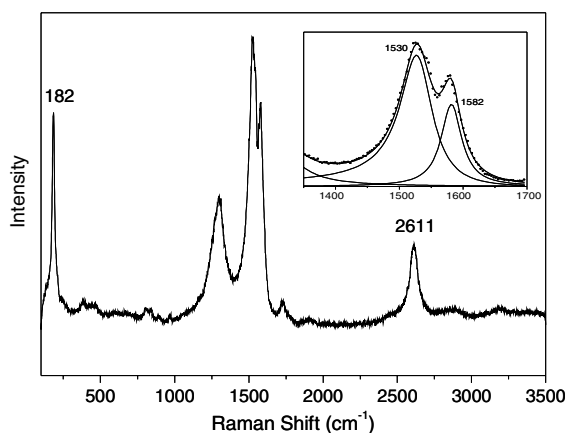


Fig. 3. Raman spectrum obtained by the subtraction of the spectrum at open circuit from the spectrum at 0.0 V, under the same conditions as Fig. 2. The inset plots the G-band fitted by two BWF lines. Their peak frequencies are indicated.
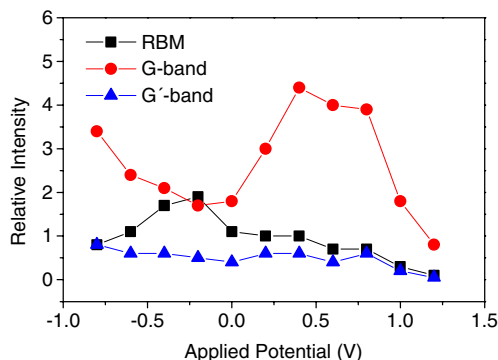
Fig. 4. Intensity of the RBM, tangential G-band and second-order G'-mode as a function of applied potential for a SWNT film cast on a platinum surface in $K_2SO_4$ 0.5 mol $L^{-1}$ aqueous solution. $E_{laser} = 1.96$ eV.

is reached, but they do so differently because of the nature of the mode.

There are a number of factors that need to be considered for understanding the intensity plots in Fig. 4. First, there are different resonance conditions for the scattered photon for the different vibrational modes. While the difference between the energy of the incident and scattered photons is ca. 0.2 eV for the tangential G-band, it is only of ca. 0.02 eV for the RBM. So, the scattered photon also plays a role in the resonance process, and scattered photons will obey different resonance conditions for the different vibrational modes. Therefore, different diameter tubes may be responsible for the RBM and tangential G-mode features of the same Raman spectrum. These different tubes will be brought in and out of resonance at different applied potentials. Second, the RBM intensity profile corresponds to the resonance of a specific SWNT, while the tangential G-mode intensity profile can be associated with the diameter distribution of the sample. The tangential G-mode intensity profile shows a maximum intensity at $V_{ap} \sim 0.6$ V, and shows a fairly symmetrical intensity quenching for positive and negative potentials. This seems to be associated with a resonance window related to the width of the diameter distribution of the nanotubes in the sample.

The data in Fig. 4 can be used to estimate the small magnitude of the shift of the $E_{ii}$ with $V_{ap}$: around 0.4 V, all features (RBM, G-band and G'-band) have a local maximum, related to resonance with the incident laser. When the applied voltage decreases, the Raman cross section increases due to a resonance processes involving $E_{ii} - E_{phonon}$. This happens around −0.2 V for the RBM, and at much lower (off scale) $V_{ap}$ for the G and G' bands. Thus, it can be concluded that a change in the electrochemical potential of 0.6 V results in a change in $E_{ii}$ of 0.02 eV, i.e. the dependence of $E_{ii}$ on $V_{ap}$ is estimated to be 0.033 eV/V.

In addition, according to resonant Raman theory, modes that have larger enhancement factors are expected to be more sensitive to a change in the resonance condition. That seems to be the case for the RBM band and also for the BWF lineshape associated with metallic tubes, and is a significant finding of the present work. This explains why these features increase more than the G' band when a good resonance condition is achieved.

### 3.3. Comparison of electrochemical behavior in different electrolytes

In order to investigate the dependence of the doping process on the chemical nature of the intercalated ion, it is interesting to compare the changes in intensity and frequency of the most important Raman features induced by the charge transfer in different electrolytes. The observed differences would then indicate a reaching of $E_{11}^{M}$ at a different $V_{ap}$ for each electrolyte, and/or that there is a significant dependence of the charge transfer and intercalation process on the chemical nature of the media. The plots in Fig. 5 show that the trends for $K_2SO_4$ and $H_2SO_4$ are qualitatively similar, yet that for $HNO_3$ is different.

In the $K_2SO_4$ media, the changes in G-band frequency (see Fig. 5a) show a charge transfer of electrons for negative potentials (below −0.4 V) while for positive potentials, hole charge transfer above +0.6 V occurs. The energy between −0.4 and +0.6 V may correspond to the region of constant DOS, while the energy below 0.4 V may correspond to emptying states and above 0.6 V to filling of states. The slopes for holes and electrons are quite similar. In the nitrate media, a significant upshift of the G-band frequency occurs for more positive potentials (at $V_{ap} \sim 0.8$ V) as compared to the sulfate media.

A similar behavior is seen when we analyze the dependence of second order G'-band frequency on $V_{ap}$ (Fig. 5b). The G' behavior of $H_2SO_4$ and $K_2SO_4$ is quite similar, but it is different for $HNO_3$. While the slopes are very similar for $H_2SO_4$ and $K_2SO_4$, a significant upshift of this band in the $HNO_3$ media with increasing applied potential only takes place for $V_{ap} > 0.8$ V. For positive $V_{ap}$, holes are introduced in the density of states of nanotubes, and anions intercalate. This would account for the similar behavior observed in $H_2SO_4$ and $K_2SO_4$, as compared to $HNO_3$: sulfate anions might intercalate more easily than nitrate ions into SWNTs bundles, and a more effective charge transfer takes place in the sulfate media.

For the sulfate, there seems to be a discontinuity in slope at 0.2 V and again at 1.0 V, which we tentatively identify with the occupation or depletion of a new subband [5]. For the nitrate, the discontinuity happens at 0.8 eV. This behavior indicates that the reaching of vHSs occurs at a different value of $V_{ap}$ in different electrolytes.
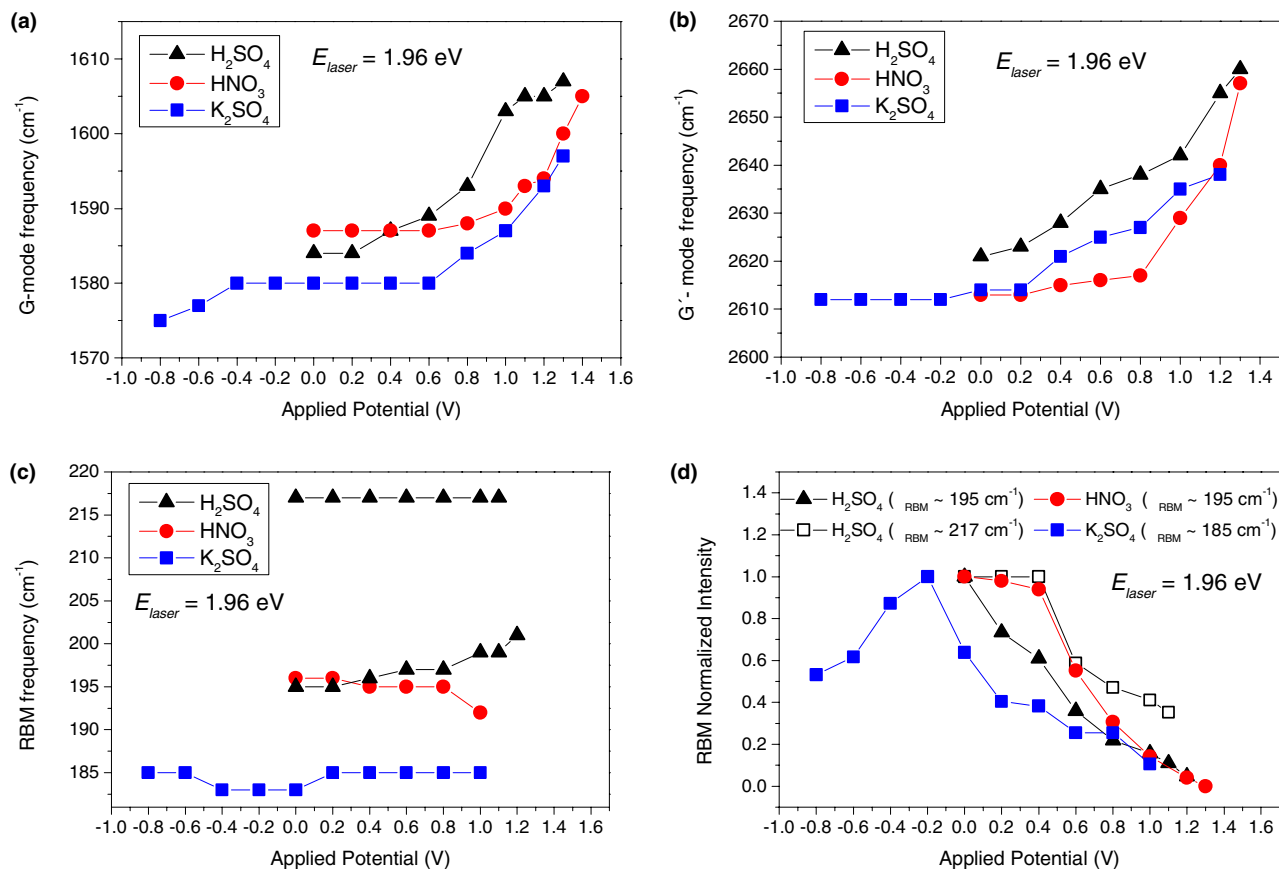
Fig. 5. Wavenumber of the (a) tangential G-band (b) second order G′-band (c) RBM band and (d) intensity of RBM band for a SWNT film in different electrolyte media as a function of the applied potential for $E_{laser} = 1.96$ eV.

In $K_2SO_4$ media, the $V_{ap}$ dependence can be analyzed over a broad range of $V_{ap}$, as compared to data obtained in acid media. While the G′-mode frequency does not shift significantly for negative applied potentials, a significant upshift occurs for $V_{ap}$ more positive than 0.2 V. Once more, an asymmetry between anodic and cathodic polarization is observed. In addition, these data also indicate that, for positive applied potentials the electronic density of the nanotubes can be easily reduced by a charge transfer process, whereas for negative applied potentials, electrons cannot be so promptly transferred to the nanotubes, probably due to the electronic repulsion. Thus the observed asymmetry in the charge transfer process might be due to an asymmetry in the density of states, but other factors cannot be ruled out at this point.

Fig. 5c,d show the dependence of the RBM intensity and frequency as a function of $V_{ap}$. The frequency shifts of the RBM bands with applied potential are extremely small as compared to the shifts in other Raman features (tangential G-band and G′-band). On the other hand, the RBM feature shows strong changes in intensity with $V_{ap}$, as reported in Fig. 5d, that depend significantly on the electrolyte.

The potential where the maximum intensity of the RBM band occurs clearly depends on the nanotube diameter. This behavior has already been reported, and indicates that the Raman effect associated with the electrochemical doping of SWNTs is itself a diameter selective process [6,13,14]. It is, however, very interesting to compare the data for the 1.27 nm tube ($\omega_{RBM} = 195$ cm$^{-1}$) and the narrower 1.14 nm diameter tube ($\omega_{RBM} = 217$ cm$^{-1}$). While the RBM feature associated with the wider diameter tube decreases sharply in intensity for applied potentials more positive that 0.0 V, for the narrower tube this effect can only be observed for $V_{ap} > 0.4$ V. The 1.27 nm tube was probed for two different electrolyte conditions ($H_2SO_4$ and $HNO_3$), and it was verified that the same behavior is observed. We interpret this result to imply that the highest energy occupied vHS for this particular diameter metallic nanotube is crossed at $V_{ap} = 0.4$ V.

## 4. Conclusions

The effect of downshifting or upshifting the Fermi level ($E_F$) by the electrochemical removal or the addition

of electrons on the resonant Raman scattering has been investigated. The vHS-related resonance condition significantly changes the intensity of the RBM and G-band and G′-band features. Experiments in both sulfate and nitrate media showed that a more effective charge transfer takes place in the sulfate media, indicating that $SO_4^{2-}$ or $HSO_4^-$ anions might intercalate more easily than nitrate ions into SWNTs bundles. These experiments also demonstrated that the reaching of vHSs happens at a different value of $V_{ap}$ in different electrolytes. It was verified that the dominant effect of the application of a gate voltage to a carbon nanotube bundle is the loss of resonance effect due to a quenching of optical transitions, but other smaller effects also need to be considered. By applying an electrochemical potential, the positions of vHSs in metallic tubes can be perturbed, resulting in a measureable change in $E_{11}^M$. As a consequence, we observed that a small change in $V_{ap}$ can be enough to bring one tube into an excellent resonance condition, and to thus get a significantly enhanced resonance Raman effect. The magnitude of the shift of the $E_{ii}$ with $V_{ap}$ was estimated to be 0.033 eV/V. In addition, the data presented in this paper confirmed that the electrochemical doping of SWNTs is itself a diameter selective process. Finally, we have confirmed that the movement of the Fermi level directly changes the charge density in metallic tubes and affects the BWF line intensity, providing a sensitive experimental probe of plasmon effects in the lineshape of the tangential G-mode in SWNT bundles.

## Acknowledgements

## References

[1] G.U. Sumanasekera, J.L. Allen, S.L. Fang, A.L. Loper, A.M. Rao, P.C. Eklund, J. Phys. Chem. B 103 (1999) 4292.

[2] L. Kavan, P. Rapta, L. Dunsch, M.J. Bronikowski, P. Willis, R.E. Smalley, J. Phys. Chem. B 105 (2001) 10764.

[3] M. Stoll, P.M. Rafailov, W. Frenzel, C. Thomsen, Chem. Phys. Lett. 375 (2003) 625.

[4] L. Kavan, L. Dunsch, Chem. Phys. Chem. 4 (2003) 944.

[5] P. Corio, P.S. Santos, V.W. Brar, Ge.G. Samsonidze, S.G. Chou, M.S. Dresselhaus, Chem. Phys. Lett. 370 (2003) 675.

[6] L. Kavan, L. Dunsch, Nano Lett. 3 (2003) 969.

[7] S. Cronin, R. Barnett, M. Tinkham, S.G. Chou, O. Rabin, M.S. Dresselhaus, A.K. Swan, S. Ünlü, B.B. Goldberg, E. Demler, Appl. Phys. Lett., in press.

[8] P. Corio, M.L.A. Temperini, P.S. Santos, J.V. Romero, J. Huber, C.A. Luengo, S.D.M. Brown, M.S. Dresselhaus, G. Dresselhaus, M.S. Dantas, C.F. Leite, F. Matinaga, J. Gonzalez, M.A. Pimenta, Chem. Phys. Lett. 350 (2001) 373.

[9] C.Y. Jiang, K. Kempa, J.L. Zhao, U. Schlecht, U. Kolb, T. Basche, M. Burghard, A. Mews, Phys. Rev. B 66 (2002) 161404(R).

[10] S. Bandow, S. Asaka, Y. Saito, A.M. Rao, L. Grigorian, E. Richter, P.C. Eklund, Phys. Rev. Lett. 80 (1998) 3779.

[11] R. Saito, G. Dresselhaus, M.S. Dresselhaus, Physical Properties of Carbon Nanotubes, Imperial College Press, London, 1998.

[12] A. Claye, S. Rahman, J.E. Fischer, A. Sirenko, G.U. Sumanasekera, P.C. Eklund, Chem. Phys. Lett . 333 (2001) 16.

[13] A. Kukovecz, T. Pichler, R. Pfeiffer, H. Kuzmany, Chem. Commun. (2002) 1730.

[14] A. Kukovecz, T. Pichler, C. Kramberger, H. Kuzmany, Phys. Chem. Chem. Phys. 5 (2003) 582.